ISSN: 2319-5967
ISO 9001:2008 Certified
International Journal of Engineering Science and Innovative Technology (IJESIT)
Volume 2, Issue 1, January 2013

# FRP-Reinforced Concrete Beams Under Combined Torsion and Flexure

Esam El-Awady[1], Mohamed Husain[2], Sayed Mandour[3]
[1] Asso. Prof., 2Asso. Prof., [3] Graduate Student, Faculty of Engineering, Zagazig University, Zagazig

***Abstract*— Concrete structures reinforced with normal steel bars experience durability problems in aggressive environments. Reinforcing bars manufactured from fiber-reinforced composites made of resin impregnated fibers (FRP) introduces a practical corrosive resistant substitute to conventional steel bars in concrete structures in aggressive environments. This paper introduces an experimental as well as analytical investigation of the torsional behavior of FRP-reinforced concrete beams. Eighteen test beams reinforced by FRP and normal steel bars were constructed and tested under combined torsion and flexure. For the sake of comparison, the tested beams in addition to ten extra beams were numerically analyzed via ANSYS software. Load-deflection relations as well as torsion-twist angle relations are drawn and a behavior comparison is undertaken. The results are then used to reach an empirical design formula that is then compared with the Egyptian code prediction.***

***Index Terms*— Concrete Beams, Fiber Reinforced Polymers, FRP Rebars, Carbon Fiber Bars, CFRP Bars, Glass Fiber Bars, GFRP Bars, Torsion.**

## I. INTRODUCTION

Conventional steel - reinforced concrete structures has durability problems in aggressive environments. They suffer steel corrosion leading to concrete cracking and spalling, which require costly maintenance. Reinforcing bars manufactured from composite materials such as fiber reinforced plastics (FRP) made of resin impregnated fibers are rapidly becoming an economic alternative for steel in concrete structures in aggressive environments all over the world [1-8]. Moreover, unlike steel bars, FRP bars have notable transparency to telecommunication waves. Glass fiber reinforced polymer (GFRP) and carbon fiber reinforced polymer (CFRP) are commonly used in as reinforcing bars. Numerous experimental and analytical researches on the FRP-reinforced concrete have been going on to gain knowledge about its behavior under different loading conditions [9-13]. No researches on the torsional resistance of FRP-reinforced concrete members (although important) have been found in literature. Furthermore, FRP-reinforced concrete codes have little or no guidance on the subject [1-5]. Many countries have recently adapted design guidelines for the design of FRP-reinforced concrete [1-5]. Many of these guidelines are based on solid literature of experimental and analytical research. While others-such as torsion- are generally copied from conventional concrete codes, due to lake of solid base of research.

This paper introduces an experimental as well as analytical investigation of the torsional behavior of FRP-reinforced concrete beams. Eighteen test beams reinforced by FRP and normal steel bars were constructed and tested under combined torsion and flexure. For the sake of comparison as well as to extend the investigative work, the tested beams were numerically analyzed via ANSYS software. The objectives of this research are to study the behavior of FRP-reinforced concrete beams reinforced by FRP bars under combined torsion and flexure, highlight the behavior weaknesses, and devising techniques to improve it. Also, introduce recommendations and guidelines for design engineers and code officials.

## II. EXPERIMENTAL PROGRAM

The Experimental program consists of eighteen test beam specimens. The specimens shape, dimensions and setup were chosen to create the required forces (Torsional moment + Bending Moment) on the test zone, The cross–sectional dimensions of the test region for all specimens are 10320 cm, and the length is 100 cm, while the total length of the specimen was 200 cm, the concrete cover for all beams 1.50 cm. Figure 1 presents the concrete dimensions, sections, and the reinforcement for B2. The eighteen specimens are divided into six groups. Group1 incorporates four reference beams, B1, B2, B3 and B4 reinforced by normal steel bars with different cases, each one represented a torsional resistance case for the beam. Groups 2 include three beams B5, B6, and B7 contain steel bars as flexural reinforcement with steel stirrups and longitudinal torsion GFRP reinforcement. Group 3 contains B8, B9, B10, and B11 reinforced by GFRP as flexural and torsional reinforcement. Group 4 includes B12,

ISSN: 2319-5967
ISO 9001:2008 Certified
International Journal of Engineering Science and Innovative Technology (IJESIT)
Volume 2, Issue 1, January 2013

B13, and B14 with GFRP bars as flexural reinforcement, GFRP ordinary stirrups, and longitudinal torsional steel bars. Group 5 comprises B15, and B16 with GFRP bars as flexural reinforcement, ordinary steel stirrups, and additional steel closed stirrups. Group 6 includes B17, and B18, beam B17 has steel bars as flexural reinforcement, steel stirrups, and additional CFRP longitudinal torsion reinforcement. While on the other hand, B18 has CFRP bars as flexural reinforcement and steel stirrups. Figure 2 introduces the reinforcements of specimens B 5 and B 14 respectively.

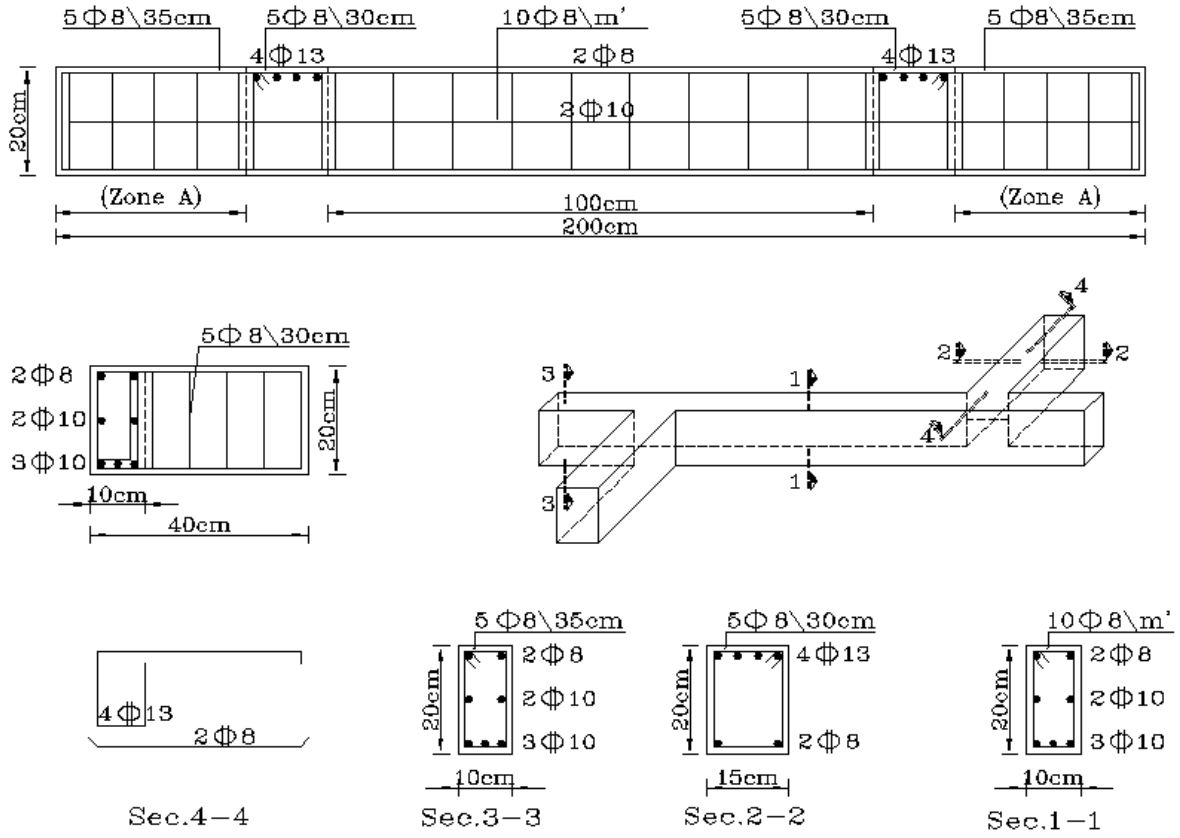


**Fig 1. Dimension and Reinforcement of Specimen**

**Fig 2. Reinforcement details of specimens B 5 and B 14**

ISSN: 2319-5967
ISO 9001:2008 Certified
International Journal of Engineering Science and Innovative Technology (IJESIT)
Volume 2, Issue 1, January 2013

All beam specimens are designed to fail in torsion. A rigid transfer steel beam is used to divide the MTS machine load onto the two tips (ends) of cantilevers. The length of cantilevers (30 cm) was chosen in order to obtain torsional moment equal to flexural moment on the test zone ( Mt = M f =P/23 0.3 ). The specimen was adjusted and then the dial guges and demcs put into the bottom surface centerline and the middle third ( top & bottom ) respectively to measure the deflection and strain records. Figure 3 shows a specimen on the test setup.
The reinforcement of each one of the two cantilevers were chosen to be 4 Φ 13 main top steel and stirrups 5 Ø 8 @ 30 cm to insure that section 2–2 can resist bending moment and shear force resulting from the loading setup. Also, the reinforcement of each of the two parts out of the test region. Section 3-3 was chosen to resist the shearing forces resulting from the loading setup. More details on the specimens and load setup can be found in Reference [13].

**Fig 3. A specimen on the MTS machine to be tested**

## III. NEUMERICAL ANALYSIS

The Commercially available structural analysis finite element program, ANSYS Nonlinear version 5.4, has been used to model and numerically analyze the tested beams. Figure 4 shows the beam model after meshing and the applied loads, the model divided into a number of finite elements with 15413 nodes.

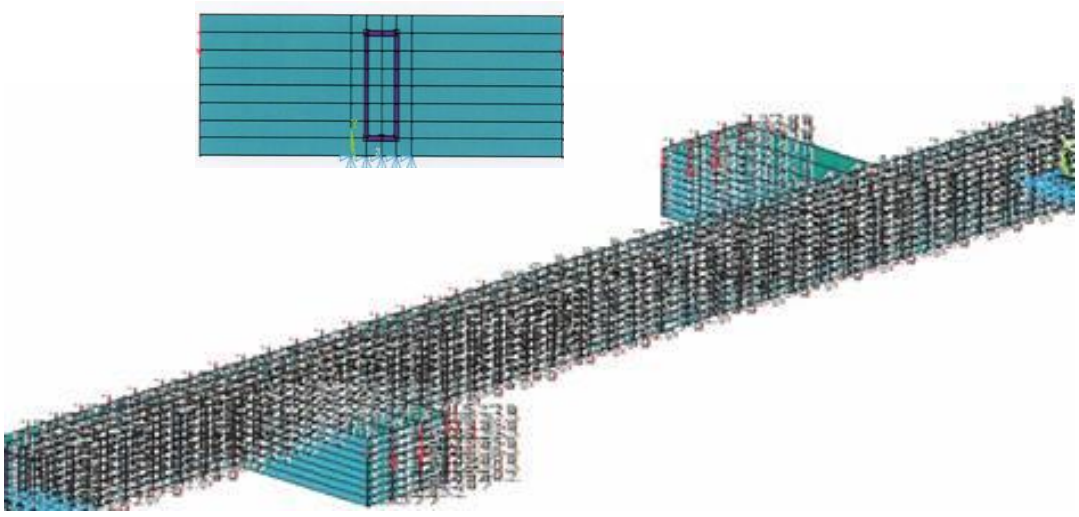

**Fig 4. Mesh distribution and applied loads**

The reinforcement was described as an elements with four types, flexural reinforcement, stirrup hangers, closed stirrups and the longitudinal torsional reinforcement, according to dimensions, shape, and modulus of elasticity. The elements were arranged to connect the related nodes, the master mesh divided into 2256 elements, while the two cantilevers were shoosed to be solid block from the steel to avoid cantilever failure during the analysis process of the program, and the same was implemented in the two supports concrete areas .

ISSN: 2319-5967
ISO 9001:2008 Certified
International Journal of Engineering Science and Innovative Technology (IJESIT)
Volume 2, Issue 1, January 2013

## IV. EXPERIMENTAL RESULTS

All tested beams failed in torsion as planned, the failure mode and cracking pattern of some of the tested beams are shown in Figure 5. The figure shows that the failure mode is torsional failure as evident of the inclined cracks develpoed in all specimens.The experimental load - midspan deflection curves are plotted for the similar torsional reinforcement arrangiments across the six groups in Figure 6, Figure 7 and Figure 8, for clear comparison. Figure 6 shows the load-deflection relations of beams reinforced with the basic flexure reinforcement only, the torsional resistance of specimen B1 (steel rienforcements) is higher than that of beams B8, B15, and B18, while it is the least ductile behavior. Beam B8 has all GFRP rienfocements, B15 has GFRP bars and steel stirrups, on the other hand B18 has CFRP bars and steel stirrups. B8 with GFRP stirrups has the lowest strength.


**Fig 5. Crack Patterns and Failure Modes Of Some Specimens**

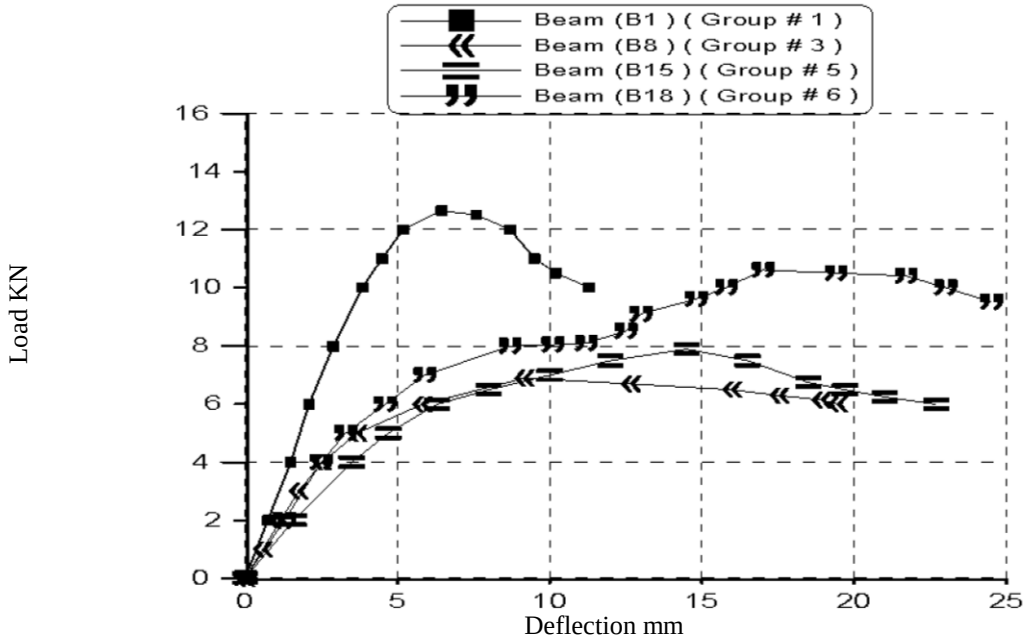


**Fig 6. Load-deflection curves for B1, B8, B15, and B18**

Figure 7 show the behavior of specimen with extra longitudinal torsion reinforcements. B2, B5, and B17 have the higher strength, while B17 has the highest ductility. They all have basic steel reinforcements, B2 has steel longitudinal torsion bars, B5 has GFRP longitudinal torsion bars, while B17 has CFRP longitudinal torsion bars. On the other hand, B9 and B12 (with basic GFRP flexure reinforcement) have the lowest strength, B9 with GFRP longitudinal torsion bars, and B12 with steel longitudinal torsion bars.

ISSN: 2319-5967
ISO 9001:2008 Certified
International Journal of Engineering Science and Innovative Technology (IJESIT)
Volume 2, Issue 1, January 2013

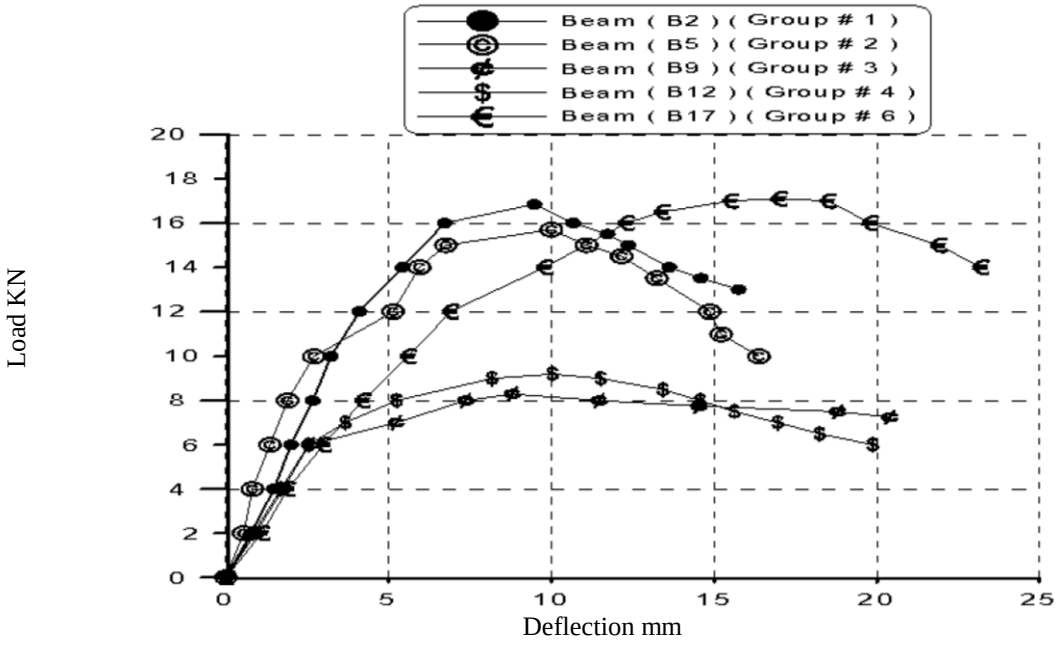


**Fig 7. Load-deflection curves for B2, B5, B9, B12, and B17**

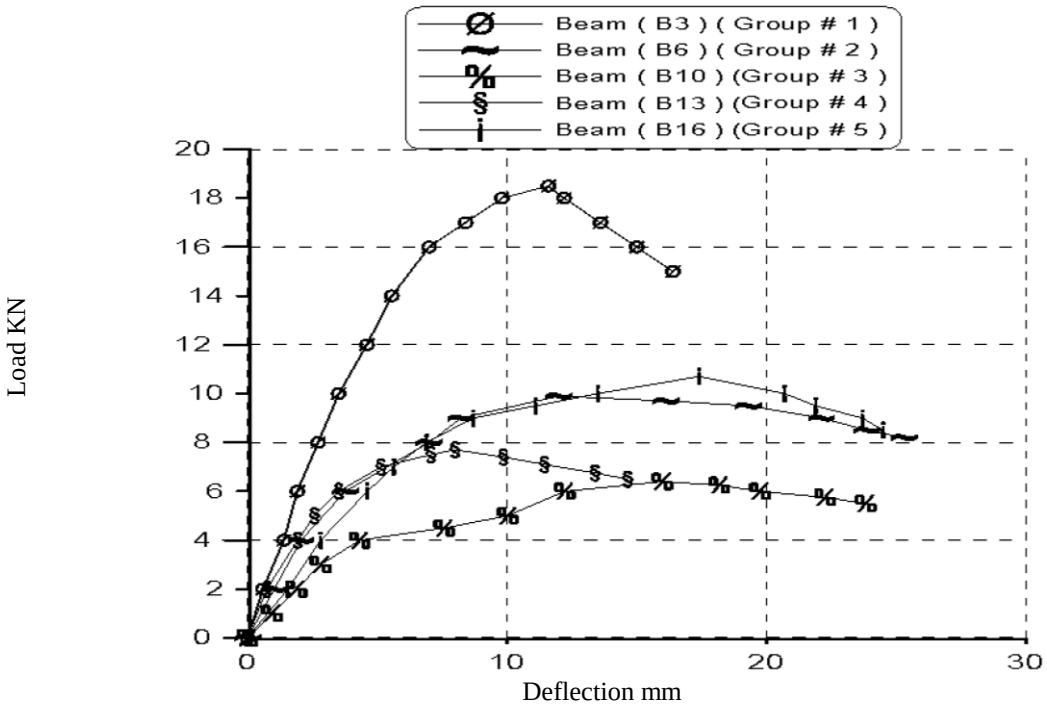


**Fig 8. Load-deflection curves for B3, B6, B10, B13, and B16**

Beam B3 has the higest strength among the tested beams as demonistrated by Figure 8, which in addition to basic steel reinforcements, has steel torsion resisted stiruups without torsional resisted longitudinal bars. On the other hand B10 has the lowest strength it has GFRP torsion resisted stiruups. For more information and analyses on the experimental results refer to Reference [13].

ISSN: 2319-5967
ISO 9001:2008 Certified
International Journal of Engineering Science and Innovative Technology (IJESIT)
Volume 2, Issue 1, January 2013

## V. NUMERICAL RESULTS

The main cracks lead to failure were found in the test zone., Figure 9 presents the deformed shape for beam B1. The stress distribution of beams B1 and B3 are introduced in Figure 10, Their torsion moment -twist angle are plotted in Figure 11.

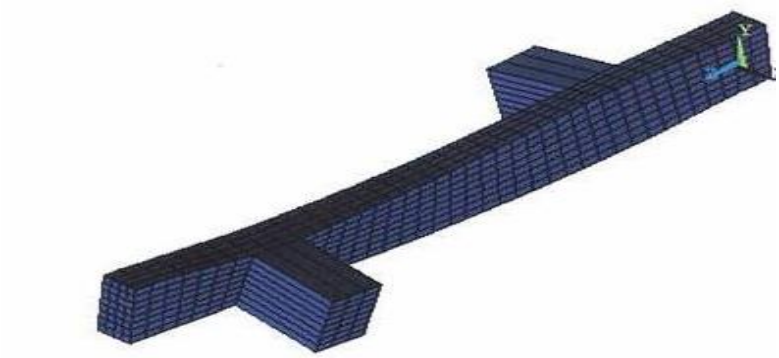

**Fig 9. Deformed shapes of beam B1**

Figure 11 shows that the angle of twist is directly proportional to the applied torque, it also demonstrate the higher torsional strength and ductility of specimen B3 which has an additional steel closed stirrups.

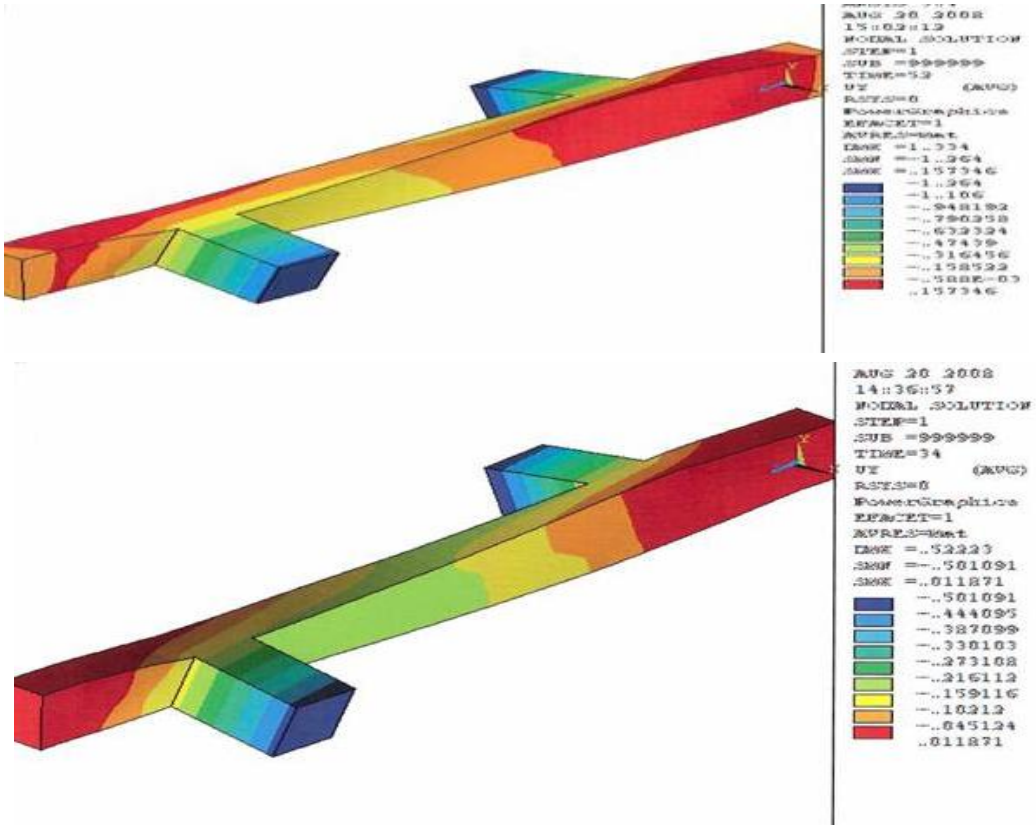

**Fig 10. Stress distribution for beams B1 and B3**

ISSN: 2319-5967
ISO 9001:2008 Certified
International Journal of Engineering Science and Innovative Technology (IJESIT)
Volume 2, Issue 1, January 2013

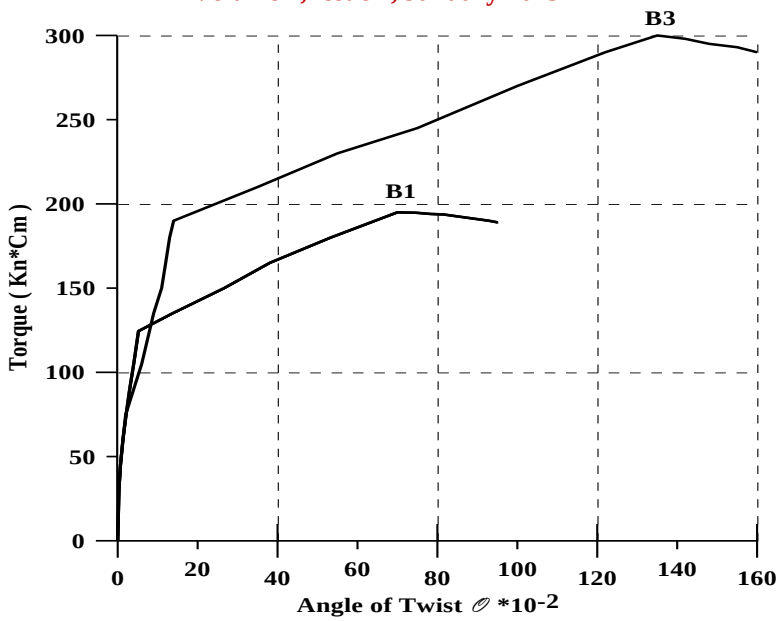


**Fig 11. Torsional Moment - Angle Of Twist Relations For B3 & B1**

Comparison between the experimental and the numerical analysis results are carried out for the two specimens B1 and B5. Load – deflection curves for both beams from tests and from ANSYS results are drawn below in Figure 12. The numerical and analytical results are found in close agreement in torsional resistance, but there exist a little discrepancy in deformations.

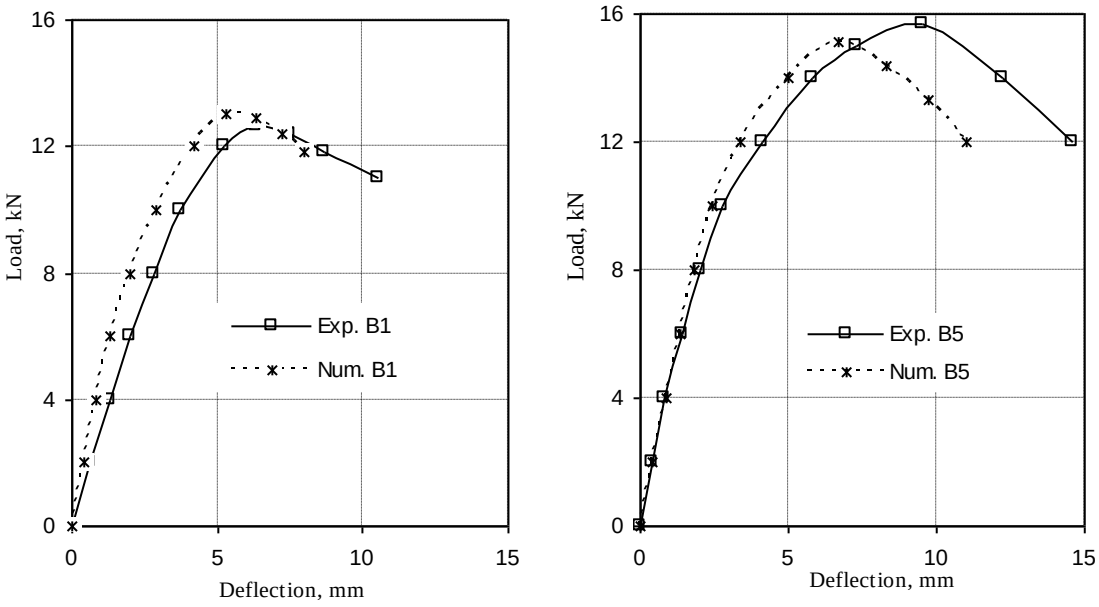


**Fig 12 Load Deflection Curves Of B1 and B5 Experimental Versus Analysis**

Additional finite element models (B5` to B27) are needed obtain more behavioral data, and to study the effect of changes in the additional longitudinal GFRP of the specimen torsional behavior. Therefore, two specimens groups (7A, and 7B) were added, each group contains five beams with the same dimensions, main reinforcement and with different longitudinal GFRP bars, Table 1 presents the additional beams.

ISSN: 2319-5967
ISO 9001:2008 Certified
International Journal of Engineering Science and Innovative Technology (IJESIT)
Volume 2, Issue 1, January 2013

**Table 1. The Additional Finite Element Models**

| Group No. | Group Name | Specimen No. | Main Reinforcement | | Additional Reinfor. | | Additional Reinforcement Statistics | | Failure Torsion (KN) (Fimite Elements | Maxiconn Torsion (KN.CM) Modified Eg.Code | % | Variance |
|---|---|---|---|---|---|---|---|---|---|---|---|---|
| | | | Longitudinal | Stirrups/m² | Longitudinal | Stirrups/m² | Area (Cm²) | $\mu_t = (A_f/A) * 100$ | | | | |
| 1 | | B1 | 3ϕ10 | 5ϕ8 | - | - | - | - | 190.00 | 138.60 | 73% | 27% |
| 7 A | Main Rfint Sieel + Add GFEP Ririst | B5 | 3ϕ10 | 5ϕ8 | 2ϕ6 | - | 0.565 | 0.28% | 205.50 | 145.10 | 71% | 29% |
| | | B19 | 3ϕ10 | 5ϕ8 | 2ϕ6 | | 1.13 | 0.57% | 216.00 | 151.55 | 70% | 30% |
| | | B20 | 3ϕ10 | 5ϕ8 | 2ϕ6 | | 1.696 | 0.85% | 228.00 | 158.00 | 69% | 31% |
| | | B21 | 3ϕ10 | 5ϕ8 | 2ϕ6 | | 1.005 | 0.50% | 213.75 | 150.12 | 70% | 30% |
| | | B22 | 3ϕ10 | 5ϕ8 | 2ϕ6 | | 2.01 | 1.01% | 232.50 | 161.60 | 70% | 30% |
| 7 B | Main Rfint Sieel + Add GFEP Ririst | B23 | 3ϕ10 | 5ϕ8 | 2ϕ6 | - | 3.014 | 1.51% | 249.00 | 173.13 | 70% | 30% |
| | | B24 | 3ϕ10 | 5ϕ8 | 2ϕ6 | | 1.57 | 0.79% | 226.50 | 156.60 | 69% | 31% |
| | | B25 | 3ϕ10 | 5ϕ8 | 2ϕ6 | | 3.14 | 1.57% | 252.00 | 174.58 | 69% | 31% |
| | | B26 | 3ϕ10 | 5ϕ8 | 2ϕ6 | | 4.71 | 2.36% | 273.75 | 192.56 | 70% | 30% |
| | | B27 | 3ϕ10 | 5ϕ8 | 2ϕ6 | | 2.26 | 1.13% | 240.00 | 164.50 | 69% | 31% |

Where :- $A_f$ is the area of the additional glass fiber bars used & $A_c$ is the Area of the concrete cross section

Figure 13 introduces the obtained formula form the the current study results. The tosion resistance is drwan against the ratio of the GFRP torsion longitudinal bars ($U_f$) in the tested and analyzed beams. These results show that the torsional resistance of the beams increased as the ratio of the additional GFRP longitudinal bars increased. It should be noted here that the study results did not find torsional resistance contribution to the GFRP stirrups formed by heating GFRP bars made with thermoplastic matrix. This figure shows that at 0 % of the additional GFRP longitudinal bars, the tested beams has a considerable torsional resistance (refer to B1 result), while the torsional resistance of the beams increased as the ratio of the additional GFRP longitudinal bars increased up to a certain level, using Micosoft Excel trendline formula by a polynomial trend the curve equation could be estimated as:

$$T_u = 190 + 42\,(U_f)^{0.8}$$

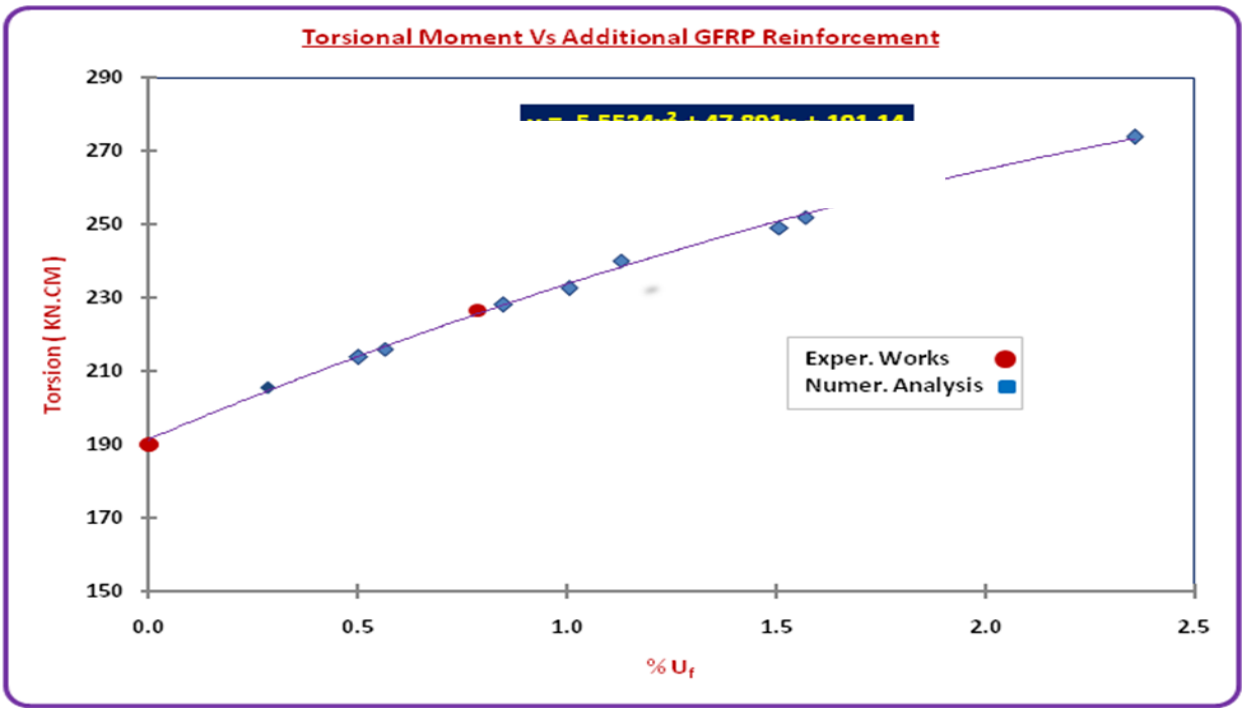


**Fig 13 Tosrion Moment Vs Ratio of the GFRP bars ( $U_f$ )**

ISSN: 2319-5967
ISO 9001:2008 Certified
International Journal of Engineering Science and Innovative Technology (IJESIT)
Volume 2, Issue 1, January 2013

There are no equations for torsion design of FRP-reinforced concrete members yet (ACI 440.1R-08) [1]. Therefore engineers currently are using the conventional steel-reinforced concrete equations in torsion design. The Egyptian code, EGP 203-2007 [4] equations of ultimate torsion strength limit state is then used for comparing the above achieved torsional strength formula. Figure 14 shows a comparison for the relation between the torsional resistance and the ratio of the additional torsional GFRP bars from the current invertigation and theone obtained from the Egyptian code, equations [4]. The figure shows that the Egyptian code, EGP 203-2007 equations underestimate the torsional resistance by about 27 % to 31.

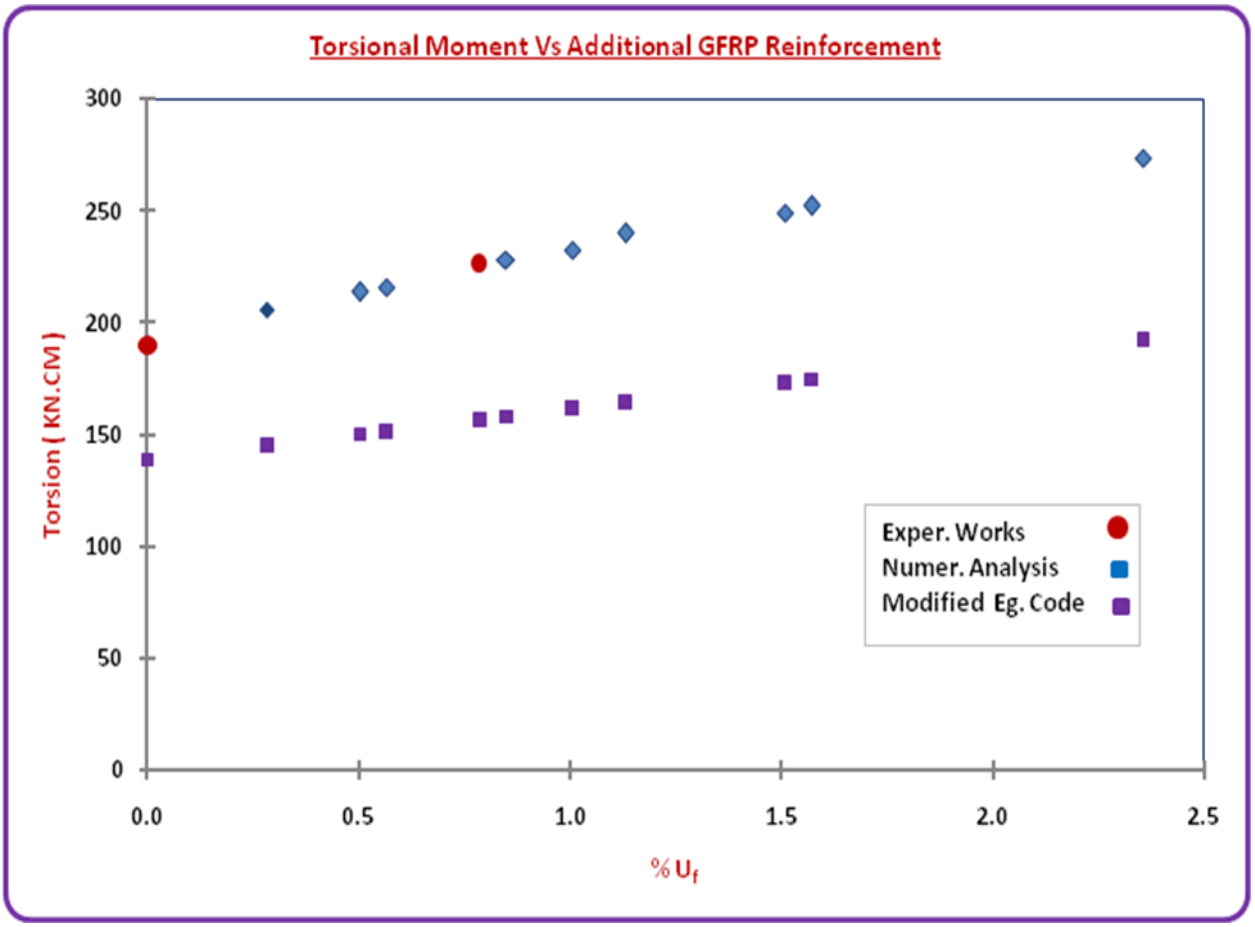


**Fig 14 Tosrional Moment Versuss Ratio Of The GFRP Bars ( $U_f$ ) By Different Solutions**

## VI. SUMMARY AND CONCLUSIONS

Eighteen test beams reinforced by FRP and normal steel bars were constructed and tested under combined torsion and flexure. They also numerically analyzed via ANSYS software in addition to ten extra models. Different reinforcement details were employed. The numerical and analytical results are found in close agreement in torsional resistance, but there exist a discrepancy in deformations. The results are then used to reach a design formula which is compared with the Egyptian code prediction. The following conclusions can be drawn: The Final Empirical Design Formula could be estimated as follows:

Tu = 190 + 42 ( Uf ) 0.8

Where; Tu in kN.cm is the maximum torsional moment for the tested beams including an additional GFRP longitudinal reinforcement . Uf is the ratio of the additional GFRP longitudinal bars relative to the beam cross-section = (Af /Ac) %, Af is the cross-sectional area of the GFRP longitudinal bars.

ISSN: 2319-5967
ISO 9001:2008 Certified
International Journal of Engineering Science and Innovative Technology (IJESIT)
Volume 2, Issue 1, January 2013

The longitudinal torsional reinforcement made from GFRP and CFRP bars have comparable effectiveness as steel in torsion reinforcements. Stirrups formed by heating GFRP bars made with thermoplastic resin are found ineffective in resisting torsion due to residual stresses on the corners arises during stirrup forming. It is recommended as a future research to use torsion resisting GFRP stirrups formed in molds with thermosetting resins.

## REFERENCES

[1] ACI 440.1R-08, "Guide for the Design and Construction of Structural Concrete Reinforced with FRP Bars," American Concrete Institute, USA, February (2008).

[2] CAN/CSA S802-02, Canadian Standards Association, Rexdale, Ontario, Canada, 177 pp., (2002).

[3] ECP 208-2005, "Egyptian Code for Design and Construction for the Fiber Reinforced polymers in Construction", Cairo, (2005).

[4] ECP 203-2007, "Egyptian Code for Design and Construction of Reinforced Concrete Structures", Cairo, (2007).

[5] JSCE, Japan Society of Civil Engineers, "Recommendations for Design and Construction of Concrete Structures Using Continuous Fiber Reinforcing Materials", Concrete Engineering Series No. 23, 325pp., Japan, (1997).

[6] Harajli, M. H., "Numerical Bond Analysis Using Experimentally Derived Local Bond Laws: A Powerful Method for Evaluating the Bond Strength of Steel Bars", ASCE, J. Struct. Engrg, V.133, Issue 5, May (2007).

[7] Nanni A., "North American design guidelines for concrete reinforcement and strengthening using FRP: principles, applications and unresolved issues," Construction and Building Materials, July (2003), 1-8 pp.

[8] Gentry, T. R. and Husain, M., "Thermal Compatibility of Concrete and Composite Reinforcements", ASCE, Journal of Composites for Construction, Vol. 3, Issue 2, May (1999), pp. 82-86.

[9] Ogasawara, T., Yokozeki, T., Onta, K. and Ogihara, S., "Linear and nonlinear torsional behavior of unidirectional CFRP and GFRP", Journal of Composites Science and Technology 67, Elsevier (2007) 3457–3464.

[10] El-Assal, A. M, Khashaba, U. A., "Fatigue analysis of unidirectional GFRP composites under combined bending and torsional loads", Journal of Composite Structures 79, Elsevier (2007) 599–605.

[11] Hanus, J. P., Shield, C. K. and French, C. W., "Development Length of GFRP reinforcement in Concrete Bridge Decks," Final Report Prepared, Published by Minnesota Department of Transportation. July (2000).

[12] Tang, W. C. Lo, T. Y. and Balendran, R. V., "Bond performance of polystyrene aggregate concrete (PAC) reinforced with glass-fiber-reinforced polymer (GFRP) bars", Journal of Building and Environment 43 (2008) 98–107.

[13] Shehab, H. K., H. S., El-Awady, M., Husain, M., and Mandour, S., "Behavior of Concrete Beams Reinforced by FRP bars under Torsion", proceedings of the 13th ICSGE, Cairo, Egypt, December (2009).